Development and Analysis of Sponge Gourd (*Luffa cylindrica* L.) Fiber-reinforced Cement Composites

Victor A. Querido,[a] José Roberto M. d'Almeida,[a,*] and Flávio A. Silva [b]

Sponge gourd (*Luffa cylindrica* L.) fiber-reinforced cement composites were developed and analyzed. Dried sponge gourd fruit's fibrous vascular system forms a natural 3D network that can reinforce matrices in composite materials, diverting cracks along the complex array of 3D interfaces between the fibers and the cementitious matrix. To avoid fiber deterioration, the cement paste was modified by incorporating pozzolanic materials. The fibers were mechanically characterized by tensile testing of strips of the 3D natural fiber array and of single fibers extracted from the array. The fibers had an average tensile strength of 140 MPa and an average Young's modulus up to 28 GPa. Image analysis showed that the fiber spatial distribution inside the 3D network was random. The modified cement paste was characterized by its workability (flow table test) and mechanical behavior (compression and three-point bending tests), with average results of 430 mm, 62.7 MPa, and 6.2 MPa, respectively. Under bending, the cement matrix collapsed after the first crack. The sponge gourd-cement composite manufactured with 1 wt% of fibers showed an average flexural strength of 9.2 MPa (approximately 50% greater than the unreinforced matrix). Importantly, the composite also presented a limited deflection-hardening behavior. These results support sponge gourd's possible use as reinforcement in cement matrix composites.

Keywords: Lignocellulosic fibers; Sponge gourd; Mechanical properties; Cement composites

Contact information: a: Department of Chemical and Materials Engineering, Pontifícia Universidade Católica do Rio de Janeiro, Rua Marquês de São Vicente, 225, Gávea, 22451-900, Rio de Janeiro, Brazil; b: Department of Civil and Environmental Engineering, Pontifícia Universidade Católica do Rio de Janeiro, Rua Marquês de São Vicente, 225, Gávea, 22451-900, Rio de Janeiro, Brazil;
** Corresponding author: dalmeida@puc-rio.br*

INTRODUCTION

Lignocellulosic fibers have attracted considerable interest as reinforcements for cementitious matrices, especially in developing countries, because these fibers have many advantages. For example, lignocellulosic fibers are readily available in many places around the globe at low cost. Moreover, they allow energy savings in their processing and are environmentally friendly, because they are biodegradable (Agopyan 1988). According to Swamy (1990), using these fibers to reinforce slabs, roof tiles, and prefabricated materials, among other uses, helps to improve the infrastructure of developing countries.

In fact, lignocellulosic fibers can be used to produce asbestos-free fiber cement boards and other cement structures with suitable mechanical properties. For example, the tensile and flexural strength of concrete is increased by the incorporation of kenaf fibers (Elsaid *et al*. 2011). Similar behavior was observed when coconut fiber was incorporated into a cement paste (Kwan *et al*. 2014). The fibers inhibited crack initiation and propagation and acted as a stress-transfer bridge after the first crack had formed, thus avoiding brittle fractures. This is an important characteristic because multiple cracking is

the desired failure mode of fiber-reinforced cement composites, as toughness can be greatly enhanced (Naaman and Reinhardt 1996). With multiple cracks, the reinforced cement will present a quasi-strain hardening behavior instead of a brittle one (Li and Stang 2004). Silva *et al*. (2009) presented the potential use of continuous natural reinforcement to obtain a cement composite system with multiple-cracking behavior. This composite is able to bridge and arrest cracks, leading to high mechanical performance and energy absorption capacity. Sisal fibers can naturally present mechanical bond components (Silva *et al*. 2009) due to different fiber morphologies, which contribute to improved mechanical behavior. Nevertheless, the durability of natural fiber cement composites remains an issue, and proper attention should be given to the matrix design (Melo Filho *et al*. 2013).

In this respect, the fibrous vascular system of the dried fruit of sponge gourd (*Luffa cylindrica* L.) presents some interesting structural characteristics for reinforcing cement matrices. As shown in Fig. 1a, the dried sponge has a 3D array of continuous fibers forming a natural mat-like material. This 3D structure has been shown to be suitable to detour advancing cracks and to enhance the toughness of polymer matrix composites (Boynard and d'Almeida 2000). The random distribution of fibers in this material can also, in principle, reduce manufacturing costs, because fiber preparation before incorporation into the matrix will be simpler when using this natural mat. However, to the knowledge of the authors, luffa fibers have not been used to reinforce cement or concrete composites. There is also a lack of information about the mechanical properties of the fibers themselves, although luffa fibers are being used in applications where their mechanical performance is of prime interest, such as reinforcement in composites (Boynard and d'Almeida 2000; Kocak *et al*. 2015) or as scaffolds for tissues (Alshaaer *et al*. 2017).

Therefore, the objectives of this study were to characterize the tensile mechanical behavior of luffa fibers and to verify the feasibility of their use to reinforce cement matrices, describing the mechanical behavior of luffa-reinforced cement composites.

EXPERIMENTAL

The sponge gourds used in this study were obtained from a farm in the county of Itápolis (21° 35' 45" S, 48° 48' 46" W), São Paulo state, Brazil. Because the sponges had varied dimensions, including their cross sections, they were opened in the middle and pressed to obtain a lamina-like material with a fairly constant thickness (Fig. 1b).

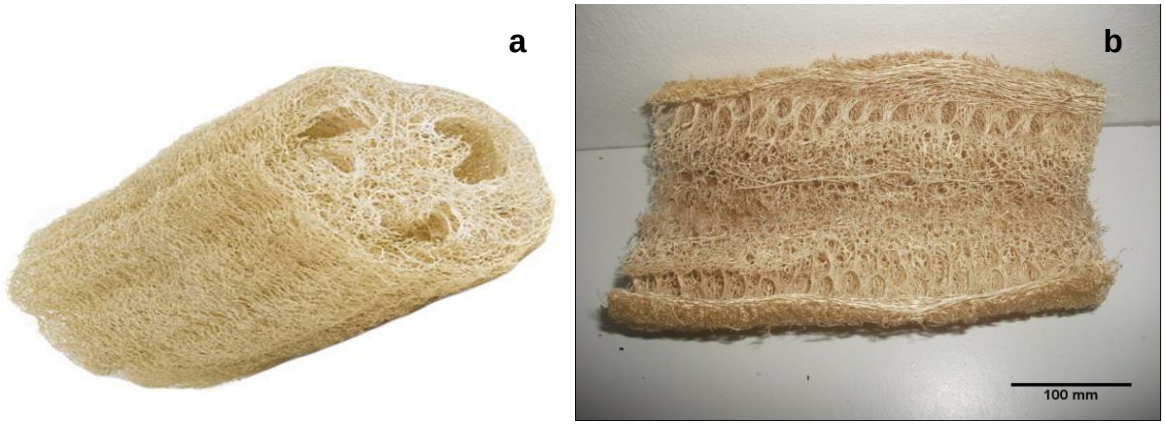

Fig. 1. The sponge, (a) before and (b) after being opened

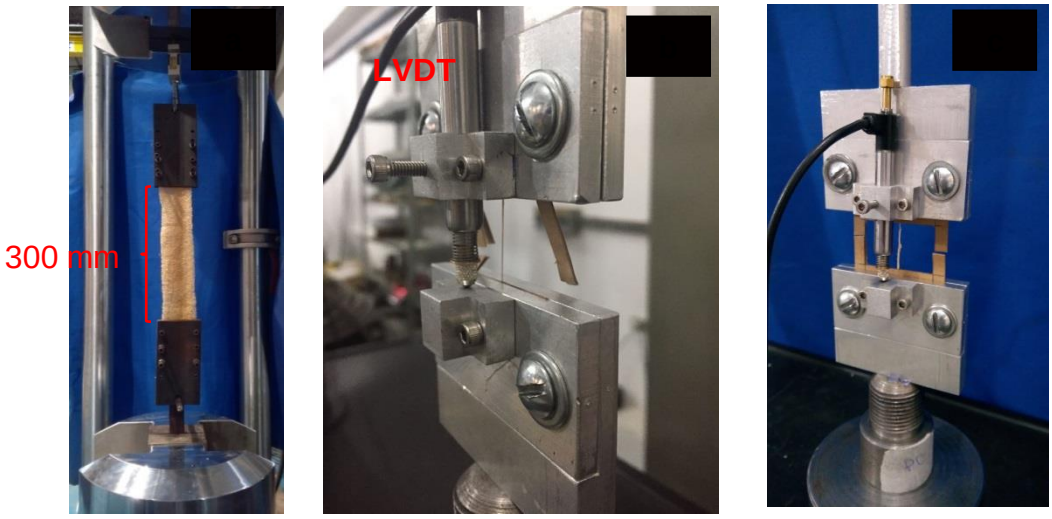

Fig. 2. Tensile testing of (a) the sponge gourd strip, (b) unbranched fibers, and (c) fibers with knots

The sponges were characterized with respect to their mechanical, morphological, and structural characteristics. Tensile tests were performed both on the sponge as a whole (using strips cut from the pressed lamina-like material) and also on individual fibers extracted from the sponges. Fifteen strips (500 mm long and 25.4 mm wide) were tested with a gauge length of 300 mm, under a displacement control rate of 0.5 mm/min. Figure 2a shows a test specimen used.

The single fibers to be tested were extracted after the sponges were opened but prior to mechanical pressing. These fibers were divided into two groups: one consisting of rectilinear and unbranched filaments and another with filaments that presented knots from branches (Fig. 2b and 2c). Ten fibers were tested per group to determine whether the presence of branches can impair the mechanical strength of the fibers. The tensile tests were performed following the recommendations of the ASTM C1557 (2014) standard. A gauge length of 20 mm was used, and the tests were performed at a displacement rate of 0.1 mm/min. The displacement was measured using a linear variable differential transformer (LVDT), as shown in Fig. 2b and 2c.

Although it is recognized in the literature that the fibers of the sponge gourd's vascular system are randomly oriented, a measure of fiber distribution has not yet been reported, to the authors' knowledge. Therefore, an analysis of the fibers' spatial distribution was performed using the plugin OrientationJ, available with the free software ImageJ/Fiji (National Institutes of Health, Bethesda, MD, USA). Images of the sponge gourd surfaces were acquired using a stereoscopic microscope (Nikon SMZ800N, Nikon Corporation, Tokyo, Japan) and were analyzed. Quantitative and qualitative measurements could be made using the software. Qualitatively, colors could be attributed to specific orientations computed by the program for each pixel of the image and correlated with angles, ranging from -90° to +90° (Fig. 3).

Quantitatively, the measurement of the orientations could be made using a discolored image, in which delimitations were made to analyze the orientations within a certain location in the image.

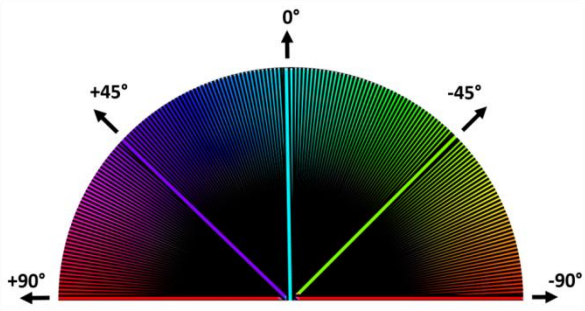

Fig. 3. Color palette that correlates colors with fiber orientation

Figure 4 shows an example of how the analysis was performed, highlighting three of the areas analyzed. The ellipses delimit the areas for spatial analysis, in which two parameters are evaluated: the preferred orientation of the fibers within the specific area and the coherence with which the fibers' angles adhere to the measured orientation. The coherence varies between 0 and 1; a value closer to 1 (100%) indicates a strong fiber coherence to the preferred orientation in the region analyzed.

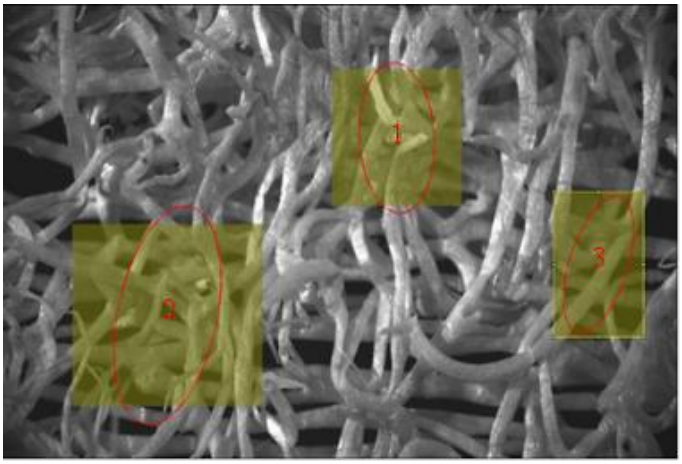

Fig. 4. Example of area delimitations to evaluate the spatial distributions of the fibers within the 3D mat of sponge gourd

The fibers were also characterized by scanning electron microscopy (SEM) and X-ray diffraction (XRD). Scanning electron microscopy was performed to observe the morphologies of the fibers and to evaluate their cross sections. Evaluation of lignocellulosic fibers' cross sections can be a source of error when the tensile mechanical properties of fibers are evaluated, as detailed in previous studies (Souza and d'Almeida 2014; Diaz *et al*. 2016). Direct measurement of the cross section by SEM has proven to be a good way to reduce errors (Diaz *et al*. 2016). The SEM analysis (JEOL JSM-6510 LV, JEOL, Tokyo, Japan) was performed on gold sputtered fibers using secondary electrons imaging at a beam voltage of 10 kV. X-ray diffraction was performed to determine the degree of crystallinity of the fibers. This is an important parameter when dealing with lignocellulosic fibers, because greater fiber crystallinity corresponds to greater chemical and thermal stability of the fiber. The analysis was performed from 5° to 80°, with steps of 0.02°/s, using CuKα (λ = 1.5406 Å) radiation at 40 kV and 30 mA.

The degree of crystallinity was calculated using the deconvolution method of the crystalline peaks and the amorphous halo (Diaz *et al*. 2016). With this method, the crystalline and amorphous areas were calculated, and then the degree of crystallinity was determined using Eq. 1 (Tserki *et al*. 2005),

$$\boldsymbol{DC} = \frac{\boldsymbol{A_c}}{\boldsymbol{A_c + A_a}} \times \mathbf{100}\% \quad (1)$$

where *DC* is the degree of crystallinity, A_c is the summation of the areas below the crystalline peaks, and A_a corresponds to the area of amorphous halo.

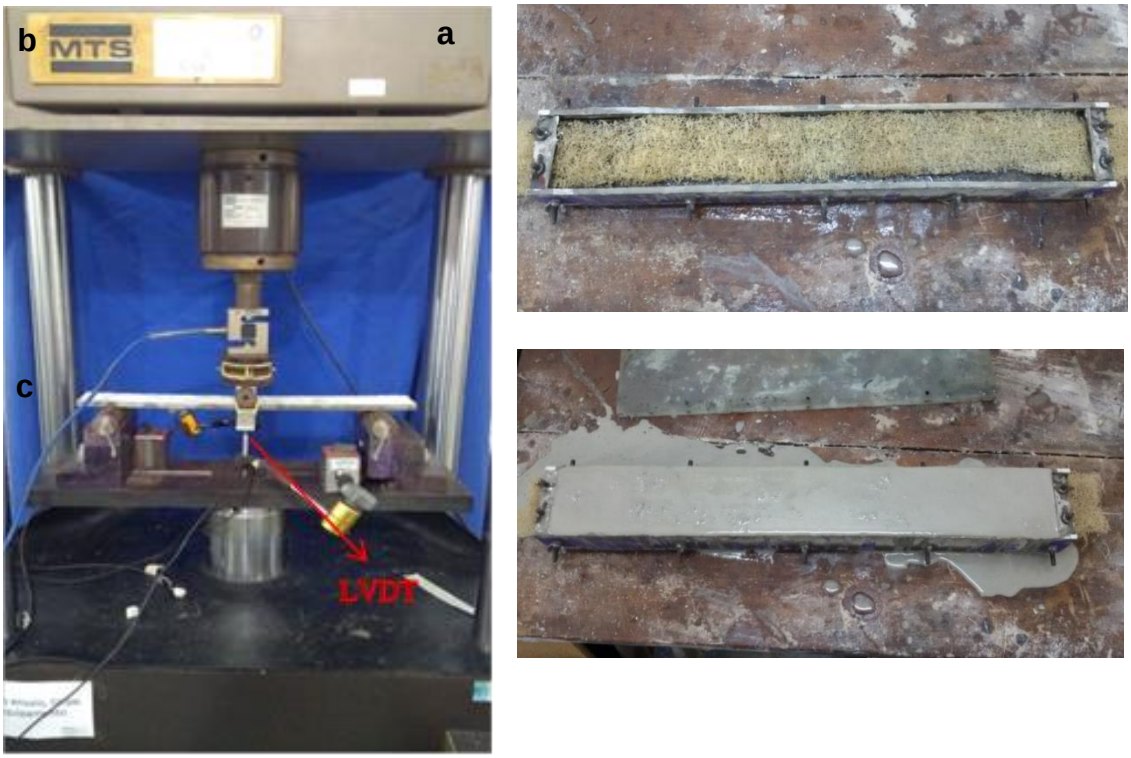

Fig. 5. Composite production and testing protocol: (a) three-point bending test and the manufacturing sequence of the sponge gourd/cement composites, in which (b) the fibers were placed inside the mold and then (c) the cement matrix was poured over the fiber layers

To manufacture the composite, the cement paste was modified using pozzolanic materials (metakaolin and fly ash) at its formulation to prevent degradation of the fibers. In fact, when using lignocellulosic fibers with a cement matrix, a strong degradation of the fibers occurs due to the chemical attack of calcium hydroxide ($Ca(OH)_2$), resulting from hydration of Portland cement (Bergström and Gram 1984). The addition of pozzolanic materials in adequate proportions into the matrix helps to prevent fiber degradation and also does not alter the mechanical properties of the final material (Silva *et al*. 2010; Fidelis *et al*. 2014). The matrix used here comprised 50 wt% of cement, 40 wt% of metakaolin, and 10 wt% of fly ash (Fidelis *et al*. 2014). The workability of this cementitious matrix was analyzed using the flow table test, following the recommendations of the Brazilian standard NBR 7215 (1996). The compressive and flexural mechanical behavior of the matrix was also analyzed. The compression test was performed using cylindrical specimens 100 mm long and with a diameter of 50 mm. The tests were performed using a compression test equipment (Controls model 50-C46Z00, Controls, Milan, Italy) (with a capacity of 2,000

kN at a stress rate of 0.25 MPa/s. Three specimens were tested after 7, 14 and 28 days (d) after molding. The displacement was measured using two transducers.

The flexural tests were performed using slabs that were 500 mm long, 60 mm wide, and 10 mm thick, using test equipment (MTS model 810, MTS, Eden Prairie, USA) with a capacity of 500 kN and a displacement rate of 1 mm/s. The displacement at the middle of the test span (400 mm in length) was monitored by two transducers (Fig. 5a). For this test, three specimens were tested only at the age of 28 d.

Slabs of sponge gourd-cement composites were manufactured with the same dimensions as the flexural specimens of the matrix, and they were tested using the same apparatus and experimental setup already described. These composites were manufactured by laying the fibers inside the mold and then pouring the cement matrix over the fiber layers (Fig. 5b and 5c). The mass fraction of fibers used was approximately 1 wt%.

RESULTS AND DISCUSSION

The tensile behavior of the sponge gourd strips is shown in Table 1, where it is compared with the behavior of an E-glass fiber plain weave fabric (d'Almeida and d'Almeida 2010) and with other lignocellulosic fabrics (d'Almeida and d'Almeida 2010; Oliveira and d'Almeida 2014). The average strength results are given as the maximum load (N) divided by areal density (g/m^2). This parameter enables different fabrics to be compared with each other and can be used to evaluate the efficiency of a fabric as reinforcement.

The tensile strengths and moduli of the single filaments are listed in Table 2. As shown, the filaments with knots had a greater tensile strength and modulus than the rectilinear, unbranched filaments. Also in Table 2, the mechanical properties of several other lignocellulosic fibers are listed for comparison (d'Almeida *et al*. 2006; Silva *et al*. 2008; Defoirdt *et al*. 2010; Souza and d'Almeida 2014; Diaz *et al*. 2016). As shown, luffa is a low-strength fiber but is a low- to high-modulus fiber. Notably, however, the results for both the tensile strength and modulus were similar to those of other lignocellulosic fibers. Interestingly, the elastic moduli of the unbranched and branched filaments were very different. It is postulated here that this difference could be due to differences in the cellulose-to-lignin ratio between the filaments, because a different amount of lignin is expected at branches than at the stalk (Ververis *et al*. 2004). However, this hypothesis must be checked. It is worth noting that an average Young's modulus of 13 GPa was measured in a previous study on sponge gourd using atomic force microscopy (AFM) (Quinayá *et al*. 2015). However, no distinction was made between branched and unbranched filaments.

Table 1. Tensile Behavior of Sponge Gourd Strips and Fabrics of Other Fibers

Fiber	Load (N)	Areal Density (g/m^2)	Strength ($N/(g/m^2)$)
Sponge gourd natural mat	151 ± 62	263	0.57
E-glass fiber plain weave fabric (d'Almeida and d'Almeida 2010)	600	223	2.70
Jute plain weave fabric (d'Almeida and d'Almeida 2010)	300	190	1.57
Ubuçu natural mat (Oliveira and d'Almeida 2014)	432 ± 112	205	2.10

± means standard deviation

Table 2. Tensile Strength and Tensile Modulus of Sponge Gourd Filaments and Other Lignocellulosic Fibers

Fiber	σ (MPa)	E (GPa)	Reference
Sponge gourd (rectilinear)	127.5 ± 75.1	3.2 ± 2.6	Present work
Sponge gourd (with knots from branches)	159.2 ± 92.2	27.9 ± 24.5	Present work
Abaca	368 – 820	15 – 23	Souza and d'Almeida (2014)
Peach palm	213	10.8	Diaz *et al*. (2016)
Sisal	396 – 696	12.8	Silva *et al*. (2008)
Coir	174 – 210	3.4	Defoirdt *et al*. (2010)
Jute	349 – 449	26.3	Defoirdt *et al*. (2010)
Piassava	118 – 144	2.4 – 2.8	d'Almeida *et al*. (2006)

σ – tensile strength; E – tensile modulus; – indicates the range of values found in the literature

The morphology of the sponge gourd is shown in Fig. 6. Figure 6a shows the 3D array of fibers, and Fig. 6b shows that the fiber has a very irregularly shaped cross section. Using the procedure of image analysis described previously in other works (Souza and d'Almeida 2014; Diaz *et al*. 2016), the average cross-sectional area measured for both branched and unbranched fibers was 0.047 mm² ± 0.017 mm². This value was well within the range measured for abaca fibers, for example (Souza and d'Almeida 2014).

The quantitative evaluation of the fiber spatial distribution inside the sponge gourd mat showed that, indeed, the fibers were randomly oriented, without any preferred orientation. Using the procedure shown in Fig. 4, the preferred orientation and coherence results for the three delimited areas are listed in Table 3. The coherence was low for all analyzed areas, indicating that there was not a preferred orientation.

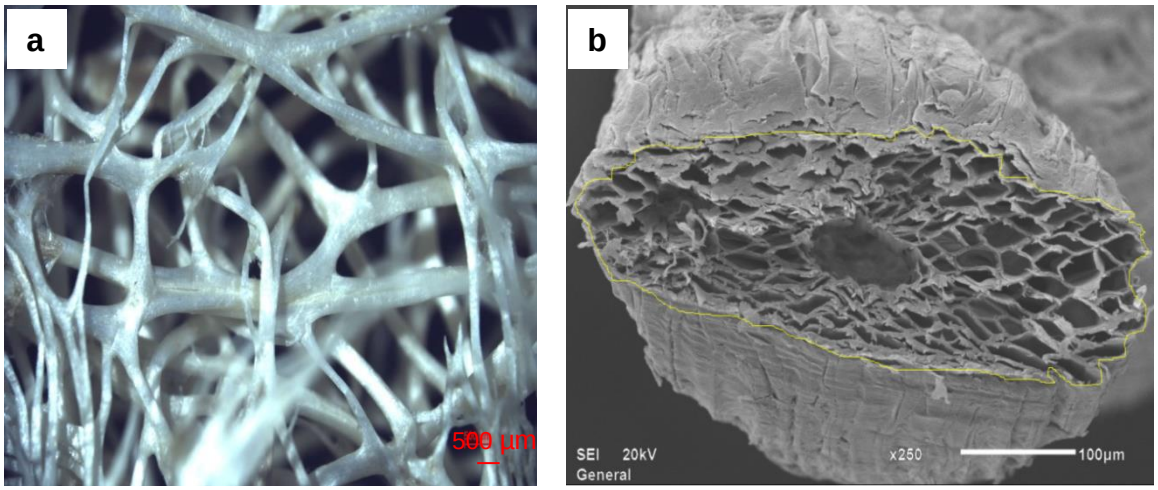

Fig. 6. (a) 3D spatial distribution of fibers inside the sponge gourd mat (optical microscopy); (b) cross section of a fiber with its perimeter highlighted for image analysis processing (SEM)

Table 3. Analysis of the Spatial Distribution of the Fibers

Area	Orientation (°)	Coherence
1	-86.3	0.30
2	77.0	0.36
3	70.6	0.39

Qualitatively, the lack of a preferred orientation is visible using the color palette (Fig. 7). The mixture of colors indicates a lack of preferential orientation of the fibers.

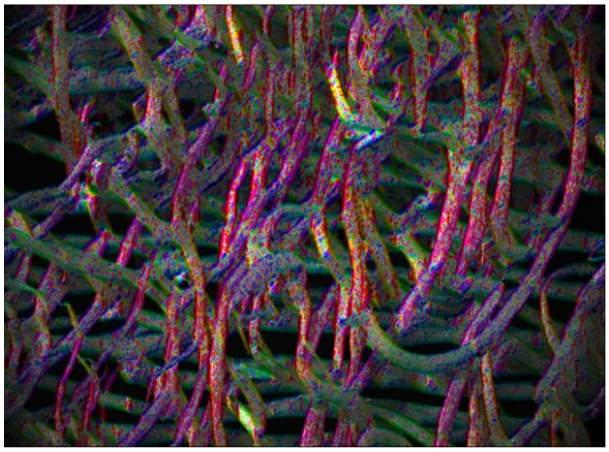

Fig. 7. Color distribution as a qualitative measurement of fiber orientation. The mixture of colors indicates lack of a preferred orientation.

The X-ray diffraction spectrum of the sponge gourd is shown in Fig. 8. The three peaks observed are due, as expected, to the diffraction of crystalline planes from native cellulose: at 15.9° the mixed signal of the (101) and $(10\bar{1})$ planes, at 22.6° the diffraction of the (002) plane, and at 34.6° the diffraction corresponding to the (040) plane (Rong *et al*. 2001). By deconvolution of the spectra, the areas of crystalline peaks and of the amorphous halo were evaluated, and the degree of crystallinity was calculated using Eq. 1. The value obtained (43%) was less than but fairly close to those reported by Adewuyi and Pereira (2017) (48.9%) and Ghali *et al*. (2009) (50%). Compared to other lignocellulosic fibers, the degree of crystallinity of the sponge gourd fibers was greater than that of palm leaf sheath fiber (30.5%) (Zhang *et al*. 2015) but less than those of abaca (65%) (Souza and d'Almeida 2014) and flax (64.1%) (Zhang *et al*. 2015).

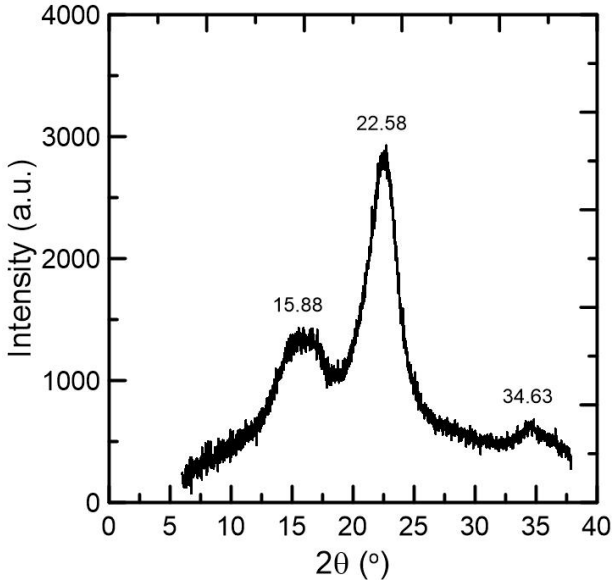

Fig. 8. X-ray diffraction spectrum of the sponge gourd

The workability of the cementitious matrix, as determined by the flow table test, was considered satisfactory. According to Silva *et al*. (2010) and Fidelis *et al*. (2014), the matrix should present a spread with a diameter of approximately 400 mm to have sufficient workability to be used in composites reinforced by natural fibers. An average value of 430 mm was obtained in this study.

The results of the compression and flexural tests of the cementitious matrix are summarized in Table 4. The value reported for the flexural strength corresponds to the opening of the first crack, and the collapse of the test specimen. The maximum deformation at this moment was 1.00 µm/mm ± 0.09 µm/mm.

Table 4. Compression and Flexural Strengths of the Cementitious Matrix

Age (d)	Compressive Strength (MPa)	Flexural Strength (MPa)
7	52.6 ± 2.3	-
14	58.7 ± 1.6	-
28	62.7 ± 0.9	6.2 ± 0.3

Barros *et al*. (2016) observed that the replacement of cement paste by 30 wt% of metakaolin and 20 wt% of calcined clay resulted in a material with a high compressive strength: 65 MPa at 28 d of age. This value corresponds well with the results obtained in this study, and it should also be highlighted that the matrix used here contained 40 wt% of metakaolin, instead of 30 wt%. Indeed, Qian and Li (2001) identified that the content of metakaolin affects the strength of concrete, and an increase of approximately 50% of the cement paste's bending strength was measured when the metakaolin content was varied between 0 wt% and 15 wt%.

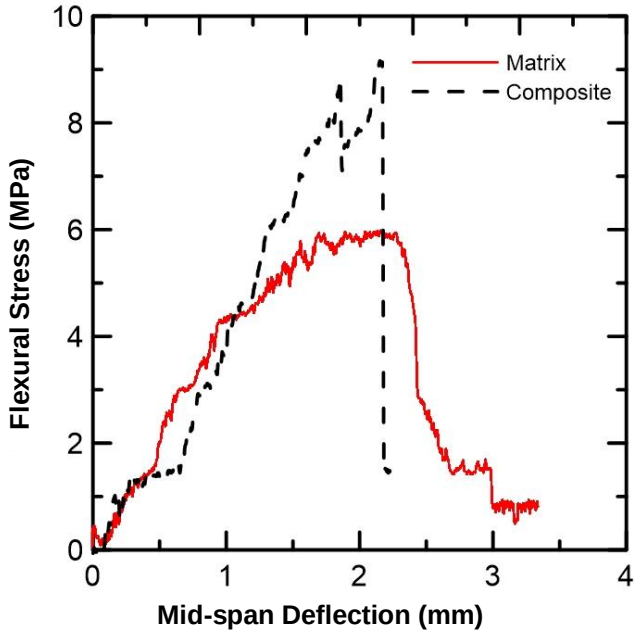

Fig. 9. Stress *vs*. deflection curves for the cementitious matrix and the sponge-gourd composite

Figure 9 shows the flexural behavior of the cementitious matrix and the sponge gourd-cement composite. The incorporation of the fibers increased the stress of the first crack by approximately 48%, from an average value of 6.2 MPa for the cementitious matrix

to 9.2 MPa for the composite. Also shown, the composite displayed a limited, but relevant, deflection-hardening effect, with a regain of resistance at the post-cracking zone. This behavior was correlated to the detour of cracks at the fiber/matrix interface, similar to what was observed when polymer-based composites were analyzed (Boynard and d'Almeida 2000).

CONCLUSIONS

1. The cement matrix used in this study, with partial replacement of the cement by pozzolanic materials, presented satisfactory compression and bending properties in its hardened state. In its fresh state, it presented suitable workability, as evaluated by the flow table test.
2. The dried vascular system of the sponge gourd presented a 3D random spatial distribution of fibers. The mechanical testing of the sponge gourd showed that this fiber was a low-strength but low- to high-stiffness fiber. Its values for these properties were similar to those of several other lignocellulosic fibers, including some fibers already used in several applications.
3. The incorporation of the fibers into the pozzolanic modified cement matrix produced a notable increase of the bending strength, although the mass fraction of the fibers used was low (approximately 1 wt%). The composites presented a limited, but important, deflection-hardening effect, indicating that the 3D distribution of the sponge gourd fibers could improve the composite toughness.

ACKNOWLEDGMENTS

The authors acknowledge the financial support from the following Brazilian agencies: the National Council for Scientific and Technological Development (CNPq – Conselho Nacional de Desenvolvimento Científico e Tecnológico) and Coordination for the Improvement of Higher Education Personnel (CAPES – Coordenação de Aperfeiçoamento de Pessoal de Nível Superior).

REFERENCES CITED

Adewuyi, A., and Pereira, F. V. (2017). "Isolation and surface modification of cellulose from underutilized *Luffa cylindrica* sponge: A potential feed stock for local polymer industry in Africa," *Journal of the Association of Arab Universities for Basic and Applied Sciences* 24, 39-45. DOI: 10.1016/j.jaubas.2016.12.003

Agopyan, V. (1988). "Vegetable fibre reinforced building materials - Developments in Brazil and other Latin American countries," in: *Natural Fibre Reinforced Cement and Concrete*, R. N. Swamy (ed.), Blackie, Glasgow, UK.

Alshaaer, M., Kailani, M. H., Ababneh, N., Abu Mallouh, S. A., Sweileh, B., and Awidi, A. (2017). "Fabrication of porous bioceramics for bone tissue applications using luffa cylindrical fibres (LCF) as template," *Processing and Application of Ceramics* 11(1), 13-20. DOI: 10.2298/PAC1701013A

ASTM C1557 (2014). "Standard test method for tensile strength and Young's modulus of fibers," ASTM International, West Conshohocken, PA, USA.

Barros, J. A. O., Silva, F. d. A., and Toledo Filho, R. D. (2016). "Experimental and numerical research on the potentialities of layered reinforcement configuration of continuous sisal fibers for thin mortar panels," *Construction and Building Materials* 102, 792-801. DOI: 10.1016/j.conbuildmat.2015.11.018

Bergström, S. G., and Gram, H.-E. (1984). "Durability of alkali-sensitive fibres in concrete," *International Journal of Cement Composites and Lightweight Concrete* 6(2), 75-80. DOI: 10.1016/0262-5075(84)90036-8

Boynard, C. A., and d'Almeida, J. R. M. (2000). "Morphological characterization and mechanical behavior of sponge gourd (*Luffa cylindrica*)–polyester composite materials," *Polymer-Plastics Technology and Engineering* 39(3), 489-499. DOI: 10.1081/PPT-100100042

d'Almeida, A. L. F. S., and d'Almeida, J. R. M. (2010). "Evaluation of the tensile and flexural mechanical behavior of hybrid glass fiber – jute fiber fabric reinforced composites," in: *Proceedings of the XII International Macromolecular Colloquium and 7th International Symposium on Natural Polymers and Composites*, Gramado, Brazil, pp. 129-133.

d'Almeida, J. R. M., Aquino, R. C. M. P., and Monteiro, S. N. (2006). "Tensile mechanical properties, morphological aspects and chemical characterization of piassava (*Attalea funifera*) fibers," *Composites Part A: Applied Science and Manufacturing* 37(9), 1473-1479. DOI: 10.1016/j.compositesa.2005.03.035

de Souza, N. C. R., and d'Almeida, J. R. M. (2014). "Tensile, thermal, morphological and structural characteristics of abaca (*Musa* textiles) fibers," *Polymers from Renewable Resources* 5(2), 47-60. DOI: 10.1177/204124791400500201

Defoirdt, N., Biswas, S., De Vriese, L., Tran, L. Q. N., Van Acker, J., Ahsan, Q., Gorbatikh, L., Van Vuure, A., and Verpoest, I. (2010). "Assessment of the tensile properties of coir, bamboo and jute fibre," *Composites Part A: Applied Science and Manufacturing* 41(5), 588-595. DOI: 10.1016/j.compositesa.2010.01.005

Diaz, J. P. V., Silva, F. A., and d'Almeida, J. R. M. (2016). "Effect of peach palm fiber microstructure on its tensile behavior," *BioResources* 11(4), 10140-10157. DOI: 10.15376/biores.11.4.10140-10157

Elsaid, A., Dawood, M., Seracino, R., and Bobko, C. (2011). "Mechanical properties of kenaf fiber reinforced concrete," *Construction and Building Materials* 25(4), 1991-2001. DOI: 10.1016/j.conbuildmat.2010.11.052

Fidelis, M. E. A., Silva, F. d. A., and Toledo Filho, R. D. (2014). "The influence of fiber treatment on the mechanical behavior of jute textile reinforced concrete," *Key Engineering Materials* 600, 469-474. DOI: 10.4028/www.scientific.net/KEM.600.469

Ghali, L., Msahli, S., Zidi, M., and Sakli, F. (2009). "Effect of pre-treatment of *Luffa* fibres on the structural properties," *Materials Letters* 63(1), 61-63. DOI: 10.1016/j.matlet.2008.09.008

Kocak, D., Mistik, S. I., Akalin, M., and Merdan, N. (2015). "The use of *Luffa cylindrica* fibres as reinforcements in composites," in: *Biofiber Reinforcements in Composite Materials*, O. Faruk and M. Sain (eds.), Woodhead Publishing, Cambridge, UK. DOI: 10.1533/9781782421276.5.689

Kwan, W. H., Ramli, M., and Cheah, C. B. (2014). "Flexural strength and impact resistance study of fibre reinforced concrete in simulated aggressive environment,"

Construction and Building Materials 63, 62-71. DOI: 10.1016/j.conbuildmat.2014.04.004

Li, V. C., and Stang, H. (2004). "Elevating FRC material ductility to infrastructure durability," in: *6th RILEM Symposium on Fibre-Reinforced Concretes (FRC)*, Varenna, Italy, pp.171-186.

Melo Filho, J. d. A., Silva, F. d. A., and Toledo Filho, R. D. (2013). "Degradation kinetics and aging mechanisms on sisal fiber cement composite systems," *Cement and Concrete Composites* 40, 30-39. DOI: 10.1016/j.cemconcomp.2013.04.003

Naaman, A. E., and Reinhardt, H. W. (1996). "Characterization of high performance fiber reinforced cement composites - HPFRCC," in: *High Performance Fiber Reinforced Cement Composites 2 (HPFRCC 2): Proceedings of the Second International RILEM Workshop*, A. E. Naaman and F. W. Reinhardt (eds.), CRC Press, London, UK, pp. 1-24. DOI: 10.1201/9781482271676

NBR 7215 (1996). "Cimento Portland – Determinação da resistência à compressão [Portland cement – Determination of compressive strength]," Associação Brasileira de Normas Técnicas, Rio de Janeiro, Brazil.

Oliveira, A. K. F., and d'Almeida, J. R. M. (2014). "Characterization of ubuçu (*Manicaria saccifera*) natural fiber mat," *Polymers from Renewable Resources* 5(1), 13-28. DOI: 10.1177/204124791400500102

Qian, X., and Li, Z. (2001). "The relationships between stress and strain for high-performance concrete with metakaolin," *Cement and Concrete Research* 31(11), 1607-1611. DOI: 10.1016/S0008-8846(01)00612-3

Quinayá, D. C. P., d'Almeida, J. R. M., and Pandoli, O. (2015). "AFM topography and quanto nanomechanical analysis of luffa lignocelullosic fibers," in: *International Scanning Probe Microscopy Rio 2015*, Armação dos Búzios, Brazil.

Rong, M. Z., Zhang, M. Q., Liu, Y., Yang, G. C., and Zeng, H. M. (2001). "The effect of fiber treatment on the mechanical properties of unidirectional sisal-reinforced epoxy composites," *Composite Science and Technology* 61(10), 1437-1447. DOI: 10.1016/S0266-3538(01)00046-X

Silva, F. d. A., Chawla, N., and Toledo Filho, R. D. d. (2008). "Tensile behavior of high performance natural (sisal) fibers," *Composites Science and Technology* 68(15-16), 3438-3443. DOI: 10.1016/j.compscitech.2008.10.001

Silva, F. d. A., Mobasher, B., and Toledo Filho, R. D. (2009). "Cracking mechanisms in durable sisal fiber reinforced cement composites," *Cement and Concrete Composites* 31(10), 721-730. DOI: 10.1016/j.cemconcomp.2009.07.004

Silva, F. d. A., Toledo Filho, R. D., Melo Filho, J. d. A., and Fairbairn, E. M. R. (2010). "Physical and mechanical properties of durable sisal fiber–cement composites," *Construction and Building Materials* 24(5), 777-785. DOI: 10.1016/j.conbuildmat.2009.10.030

Swamy, R. N. (1990). "Vegetable fibre reinforced cement composites – A false dream or a potential reality?," in: *Vegetable Plants and their Fibres as Building Materials: Proceedings of the Second International RILEM Symposium*, H. S. Sobral (ed.), Routledge, London, UK. DOI: 10.4324/9780203626818

Tserki, V., Zafeiropoulos, N. E., Simon, F., and Panayiotou, C. (2005). "A study of the effect of acetylation and propionylation surface treatments on natural fibres," *Composites Part A: Applied Science and Manufacturing* 36(8), 1110-1118. DOI: 10.1016/j.compositesa.2005.01.004

Ververis, C., Georghiou, K., Christodoulakis, N., Santas, P., and Santas, R. (2004). "Fiber dimensions, lignin and cellulose content of various plant materials and their suitability for paper production," *Industrial Crops and Products* 19(3), 245-254. DOI: 10.1016/j.indcrop.2003.10.006

Zhang, T., Guo, M., Cheng, L., and Li, X. (2015). "Investigations on the structure and properties of palm leaf sheath fiber," *Cellulose* 22(2), 1039-1051. DOI: 10.1007/s10570-015-0570-x

Article submitted: July 25, 2019; Peer review completed: September 18, 2019; Revised version received and accepted: October 14, 2019; Published: October 31, 2019.
DOI: 10.15376/biores.14.4.9981-9993